Proceedings of the ASME 2020
International Mechanical Engineering Congress and Exposition
IMECE2020
November 16-19, 2020, Portland, OR, USA

IMECE2020-23746

PASSIVE IMPEDANCE-LOADED SURFACE ACOUSTIC WAVE (SAW) SENSOR FOR SOIL CONDITION MONITORING

Jian Chu,
Department of Mechanical Engineering, New York Institute of Technology
New York, NY

Ioana Voiculescu
Department of Mechanical Engineering, City College of New York
New York, NY

Ziqian Dong
Department of Electrical Engineering, New York Institute of Technology
New York, NY

Fang Li*
Department of Mechanical Engineering, New York Institute of Technology
New York, NY

ABSTRACT

This paper presents an innovative system to monitor the physical soil conditions needed for modern agriculture. The current technique to measure soil properties relies on taking samples from place to place and takes them for laboratory testing. To build up and monitor a data-based system for a large area, such a method is costly and time-consuming. This paper reported our recent work on the development of a passive impedance-loaded surface acoustic wave (SAW) sensor for a low-cost soil condition monitoring system. The SAW sensor will eventually be connected to an antenna and a impedance-based sensor for autonomous soil nutrient sensing. In this research, first, the coupling-of-modes (COM) analysis was performed to simulate the SAW device. The sensors were fabricated with E-beam lithography techniques and tested with different external load resistances. We investigated how the sensor signal changed with the external resistance loading. The experimental results were verified by comparing them with simulation results.

Keywords: SAW sensor, Soil Condition, COM model

NOMENCLATURE

SAW	surface acoustic wave
COM	coupling-of-modes
IDT	interdigital transducer

1. INTRODUCTION

A monitor system for physical soil conditions is needed for modern agriculture.[1][2][3] The current technique to measure soil properties relies on taking samples from place to place and takes them for laboratory testing. The current methods to build up and monitor a data-based system for a large area are costly and time-consuming.

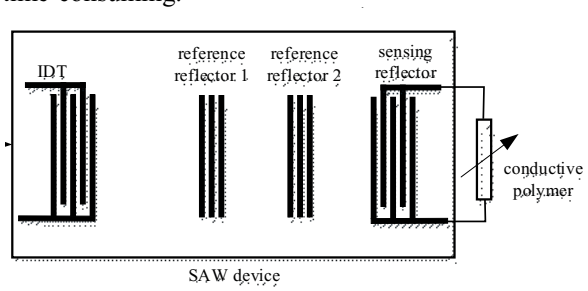

FIGURE 1. Impedance-loaded SAW sensor

The work reported in this paper is part of a project that is aimed to build a low-cost autonomous soil nutrient-sensing system that can support precision agriculture. We designed, fabricated, and tested an impedance-loaded surface acoustic wave (SAW) sensor (Figure 1). The SAW sensor consists of an interdigital transducer (IDT), which converts electrical signals to surface acoustic waves and multiple reflectors (i.e., sensing reflector and reference reflectors). The reflectors reflect the surface acoustic waves back to the IDT. The IDT port of the SAW device can be connected to a wideband antenna that receives and transmits signals between the SAW device and the ground penetrating radar (GPR). Thus the SAW device can be operated passively and wirelessly. The sensing reflector is connected to a conductive polymer-based impedance sensor to detect the nitrate and heavy metal ion concentrations in soil.

Variations in the load impedance due to the interaction between the ions and conductive polymer alter the acoustic reflection properties of the sensing reflector. By measuring the amplitude ratio of the reflected signals from the reference and sensing reflectors, the concentration of the nutrient in the soil can be measured.

In this paper, the coupling-of-modes (COM) analysis was performed to simulate the SAW device. The sensors were fabricated with electron-beam (E-beam) lithography techniques. After fabrication, we tested the sensor and investigated how the sensor signal changed with the external impedance loading. The experimental results were verified by comparing them with simulation results.

2. METHODS

2.1 Theoretical Simulation

In this study, the COM method was used to model the reflective SAW device. It provided an efficient and highly flexible approach for modeling various kinds of SAW devices[1][2][3] For the structure which has a constant mechanical periodicity, pitch p, the amplitude of two counterpropagating waves $\varphi_+(x)$ and $\varphi_-(x)$ can be written in terms of the slowly varying field R(x) and S(x):

$$\begin{cases} \varphi_+(x) = R(x)e^{-i\pi x/p} \\ \varphi_-(x) = S(x)e^{+i\pi x/p} \end{cases} \quad (1)$$

The COM equation can be written as:

$$\begin{cases} \dfrac{dR(x)}{dx} = -i\delta R(x) + i\kappa S(x) + i\alpha V \\ \dfrac{dS(x)}{dx} = -i\kappa^* R(x) + i\delta S(x) - i\alpha^* V \\ \dfrac{dI(x)}{dx} = -2i\alpha^* R(x) - 2i\alpha S(x) + i\omega CV \end{cases} \quad (2)$$

where δ is the detuning parameter given by:

$$\delta = \frac{\omega}{v} - \frac{\pi}{p} - i\gamma = \frac{2\pi(f-f_0)}{v} - i\gamma \quad (3)$$

where V is the voltage, I is the current, f_0=v/2p, and κ, α, ν, γ, C are reflectivity due to perturbations, transduction coefficient, SAW velocity, attenuation, and capacitance per unit length, respectively. The asterisk denotes the complex conjugate. To render the COM model effective, the P-matrix model has been created, an efficient modeling technique where the linear COM equation for transducers or reflectors is expressed as the elements of the matrix. The equations are shown as follows:

$$\begin{bmatrix} \varphi_-(x_1) \\ \varphi_+(x_2) \\ I \end{bmatrix} = \begin{bmatrix} P_{11}(f) & P_{12}(f) & P_{13}(f) \\ P_{21}(f) & P_{22}(f) & P_{23}(f) \\ P_{31}(f) & P_{32}(f) & P_{33}(f) \end{bmatrix} \begin{bmatrix} \varphi_+(x_1) \\ \varphi_-(x_2) \\ V \end{bmatrix} \quad (4)$$

where P_{11} and P_{22} are the reflection coefficients, and P_{12}=P_{21} is the transmission coefficient. The components P_{13} and P_{23} describe the excitation efficiency of the IDT. The components P_{31} and P_{32} measure the current generated in the IDT by the arriving waves. The P_{33} component is the admittance, describing the acoustic and electrostatic currents due to the drive voltage V. If considering the impedance of the external loading and matching circuit, the reflection coefficient P_{11} will be modified as

$$P_{11}(Z_{load}, Z_{match}) = P_{11} - \frac{P_{31} \cdot P_{13}}{P_{33} + \frac{1}{Z_{load}+Z_{match}}} \quad (5)$$

where P_{11}, P_{31}, P_{13}, and P_{33} are the components of P-matrix for IDT with zero loadings, and Z_{load} and Z_{match} are impedance of the external load and matching circuit, respectively[6]. Using the expressions of P matrix components of the IDTs, gap, and reflectors, the reflection coefficient S_{11} can be deduced [5] [6].

There are five COM parameters to be determined: velocity v, reflectivity κ_p, normalized transduction α_n, normalized capacitance C_n, and attenuation γ_p. The first four COM parameters, which were obtained through the FEM simulation with COMSOL Multiphysics, are listed in Table 1. The attenuation γ_p is assumed to be 0.001 Neper/λ_0

Parameters	Symbol	Data	Unit
Velocity	v	3800	m/s
Reflectivity	κ	0.0238	$\Omega^{-\frac{1}{2}}$
Normalized transduction coefficient	α	$7.52\text{x}10^{-4}$	$\Omega^{-\frac{1}{2}}$
Normalized capacitance	C	$48.2\text{x}10^{-11}$	F/m

TABLE 1. Parameters calculated by the FEM simulation with

2.2 Sensor Fabrication

A SAW sensor with the electrode layout shown in Figure 2 was fabricated. The sensor parameters are listed in Table 2.

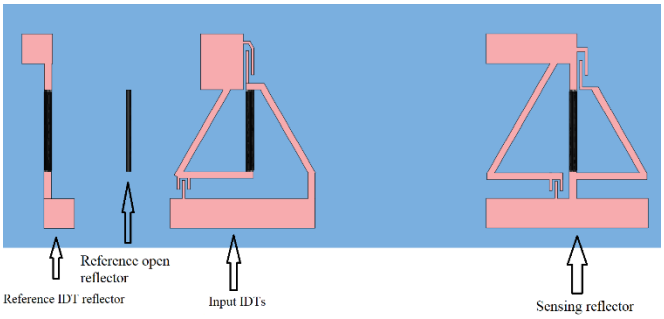

FIGURE 2. The electrode layout of the sensor, from left to right, there are the reference IDT reflector, reference open reflector, input IDTs, and sensing reflector, respectively.

Input IDTs, reference IDT reflector, and sensing reflector's finger pairs	10
Distance from Input IDTs to reference open reflector	150λ
Distance from input IDTs to sensing reflector	400λ
Distance from reference open reflector to reference IDT reflector	100λ
Reference open reflector finger pairs	5
Aperture	100λ
Wavelength (λ)	15.2um

TABLE 2. The parameters of the layout and fabricated SAW sensor

The fabrication of the sensor was performed with E-beam photolithography. The process started by the cleaning step of a YX-Cut $LiNbO_3$ (MTI cooperation) wafer that was 0.5mm thick with acetone, methanol, IPA, and DI water. After drying with nitrogen, 950 PMMA A6 photoresist (MichroChem, Newton, MA) was applied to the piece on a spin coater (Brewer Science, Rolla, MO) at 3000rpm for 45 seconds. For the protection, a thin layer of Espacer 300z (Showa Denko America), a dissipation liquid polymer, was spun on the wafer at 3000rpm for 45 seconds, then the wafer was baked for 2 minutes at 110°C. The IDTs were then fabricated with e-beam writing using the JEOL e-beam writer (JEOL JBX-6300FS Electron Beam Lithography System). After writing the pattern on the substrate, the wafer was prepared for development using MIBK: IPA 1:3 (MichroChem, Newton, MA) for 90 seconds. The next step was to deposit metal on the developed polymer. In our design, we deposited 10 nm chromium and then 90 nm gold in the e-beam evaporator (Kurt J. Lesker PVD 75 thin film deposition system). Once the deposition was completed, the wafer was ready for lift-off and was soaked in acetone on a hotplate at 60°C for 30 to 60 minutes.

Once SAW sensor chips were successfully fabricated, a wedge wire bonder (Model 4526, Kulicke and Soffa, Singapore) was used to bond wires to connect the sensor terminals to MMCX connectors soldered on a flexible printed circuit board (PCB), as illustrated in Figure 3. The connectors were then connected to the network analyzer or external impedance sensor by loading via RF cables for testing.

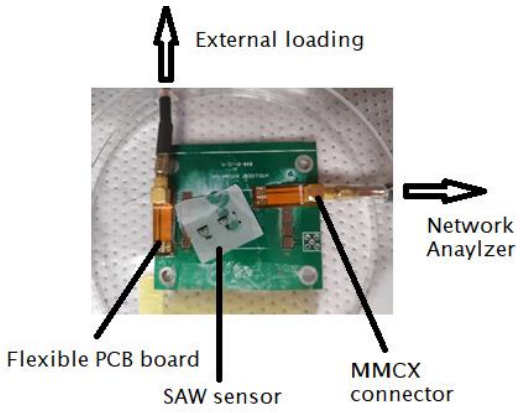

FIGURE 3. SAW sensor with connection to the network analyzer and impedance sensor

2.3 Sensor Testing

The first test experiment was completed by connecting the input IDT to an HP Network Analyzer (E5061B Aligent Technology Corporation). The measurements were done by recording the S_{11} spectrum in the frequency domain. S_{11} is a one-port reflection measurement. The measurements were saved from the network analyzer in the frequency domain. Results were saved with a bandwidth of 100MHz to ensure that all desired information could be gathered. Finally, the S_{11} was converted to signal in the time domain by inverse Fourier transform.

The second experiment is to test the SAW sensor with external resistance loading, which is to a representative of the polymer sensor. We tested three conditions, i.e., 0 ohms (short state), 50 ohms (load state), and infinite ohms (open state).

3. RESULTS AND DISCUSSIONS

The initial test was to verify if the sensor signal was strong enough. Figure 4 shows the experimental and simulation results of the S_{11} magnitude in the time domain. From left to right, the first two pulses were from the two reference reflectors, and the last one was from the sensing reflector. The time delay of each pulse is agreeable with the simulation results.

Figure 5 shows the testing results of the S_{11} magnitude in the time domain with the sensing reflector connected to different loading resistances. The magnitude of the first two pulses, which were from reference reflectors, did not change, and the signal of the third pulse, which was from the sensing

reflector, changed with external resistance loading. From the comparison of the signal difference of the second pulse and third pulse, we can get external loading information.

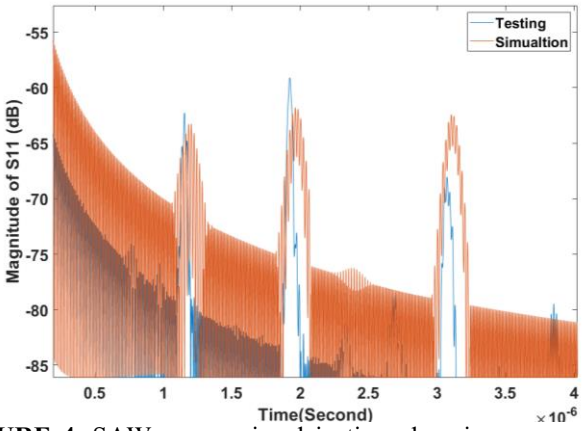

FIGURE 4. SAW sensor signal in time domain compared to simulation results.

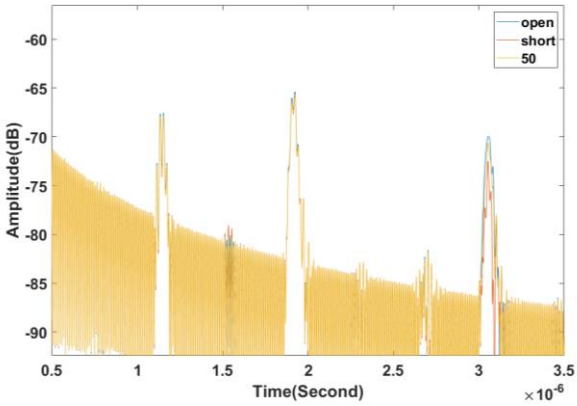

FIGURE 5. S_{11} magnitude in the time domain with the sensing reflector connected to different loading resistances

The simulation of external loading was performed from 5 ohms to 200 ohms, and the testing of external loading was 0 ohms, 50 ohms, and infinite ohms (we used 300 ohms to draw Figure 6). In the simulation results, the equation (5) does not have an impedance part of the matching circuit because we only use resistance for testing. From Figure 6, the trend of testing and simulation results was the same. The magnitude of the pulse reflected from the sensing reflector increases with the external loading resistance. The magnitude changes rapidly when the resistance is less than 50 ohms. The change rate becomes low when the resistance is larger than 50 ohms.

However, testing results showed the magnitude of the sensing pulse has a smaller shift with external loading resistance from 0 to infinity, compared with the simulation results. In future work, we will improve the sensor design to enhance the strength of the sensing pulse signal and to improve the device sensitivity.

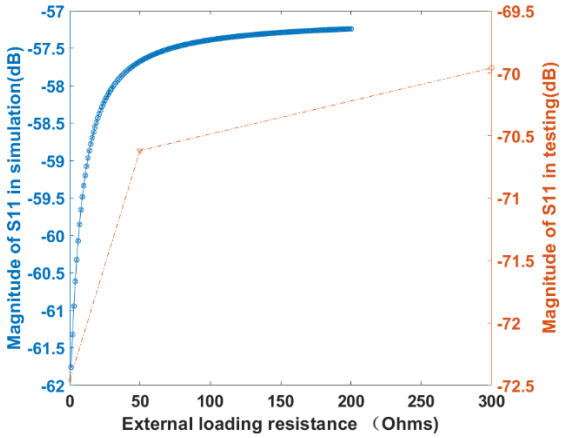

FIGURE 6 Comparison of testing and simulation results of the sensing pulse magnitude change with the external loading resistance

4. CONCLUSION

In this paper, the COM analysis was performed to simulate the SAW device. The sensors were fabricated with E-beam lithography techniques. After the sensors were fabricated, we tested the sensor and investigated how the sensor signal changed with the external impedance loading. The experimental results were verified by comparing them with the simulation results.

ACKNOWLEDGEMENTS

This material is based upon work supported by the National Science Foundation under Grant No. 1841558. Research carried out in part at the Center for Functional Nanomaterials, Brookhaven National Laboratory, which is supported by the U.S. Department of Energy, Office of Basic Energy Sciences, under Contract No. DE-SC0012704. The authors would like to thank Dr. Aaron Stein and Dr. Fernando Camino from Brookhaven National Laboratory for their comments, suggestions, and support for this research.

REFERENCES

[1] The World Bank IBRD.IDA; population data, by country. Retrieved October 20, 2015, from http://data.worldbank.org/indicator/SP.URB.TOTL.IN.ZS

[2] World Health Organization, Population Growth statistics for 2014. Retrieved October 20, 2015, from http://www.who.int/gho/urban_health/situation_trends/urban_population_growth_text/en/

[3] V. I. Adamchuk, J. W. Hummel, M. T. Morgan, S. K. Upadhyaya, “On-the-go soil sensors for precision agriculture,” Computers and Electronics in Agriculture, vol. 44, no. 1, 2004, pp. 71−91, ISSN

0168-1699,
https://doi.org/10.1016/j.compag.2004.03.002.
[4] V. Plessky, J. Koskela, “Coupling-of-modes analysis of SAW devices,” Int. J. High Speed Electron. Syst., vol. 10, pp. 867–947, 2000.
[5] Wen Wang, Keekeun Lee, Insang Woo, Ikmo Park, Sangsik Yang, “Optimal design on SAW sensor for wireless pressure measurement based on reflective delay line”, Sensors and Actuators A vol. 139, pp. 2–6, 2007.
[6] V. Plessky, J. Koskela, “Coupling-of-modes analysis of SAW devices,” *Int. J. High Speed Electron. Syst.*, vol. 10, pp. 867–947, 2000.
[7] Han, Tao; Shi, Wenkang, Surface Acoustic Wave Devices Based Wireless Measurement Platform for Sensors. Micromachining and Microfabrication Process Technology and Devices, Norman C. Tien, Qing-An Huang, 14 Editors, Proceedings of SPIE Vol. 4601 (2001)